Радиофизика и радиоастрономия, 1998, т. 3, №2, стр. 181-190

УДК 550.388

Perturbations in the Ionosphere Following U. S. Powerful Space Vehicle Launching

L. F. Chernogor, K. P. Garmash, L. S. Kostrov, V. T. Rozumenko, O. F. Tyrnov, and A. M. Tsymbal

Kharkiv State University
4 Svoboda Square, Kharkiv 310077, Ukraine

The paper is received by editor August 3, 1998, rewritten January 10, 1999

Quasi-periodic perturbations have been detected in the electron density in both the D and F regions on May 15, 1997, the day of Space Shuttle Atlantis launch. The electron density varied quasi-periodically with periods of tens of minutes during an interval of 1 to 2 hours. An attempt is made to associate the phenomena observed with possible global-scale processes in the mesosphere and lower thermosphere which accompany the launch at the beginning of the main phase of the geomagnetic storm.

Introduction

Investigations of possible effects from rocket burns on the near-earth space environment are of interest for at least three reasons. First, the release of rocket vapor trail, the transfer of momentum to the air, and the generation of acoustic and other types of waves in the gas and the plasma, as well as in the geomagnetic field and the global-scale electric field distribution, are a complex active experiment in itself. Second, these perturbations can have significant effects on the propagation of radio waves of different frequency ranges. Third, the induced disturbances and the release of matter could be of interest to ecologists.

The phenomena accompanying rocket launches are noted for their variety, spatial and temporal features, energetics, and other characteristics [1]. The energetics of these phenomena is lower only than that of the processes induced by nuclear explosions. Their classification can be conveniently made in terms of spatial scales. We call the perturbations characterized by the scale sizes $L_1 \le 100$ km, $L_2 \sim 100$ to 1000 km, and $L_3 \sim 1000$ to 10 000 km localized, large-scale, and global-scale, respectively. The localized perturbations arise as a turbulent eddy flow that occurs downstream from the body of a rocket, their properties being dependent on the rocket velocity v and the thrust F. The rocket leaves these perturbations in its wake along the rocket trajectory. The magnitude of L_1 can be estimated using the relation $L_1 = \sqrt{2F / \rho_0 v_0^2}$ where $v_0 \approx v$, v_0 and ρ_0 are the velocity and the mass density of incoming undisturbed air flow, respectively. As ρ_0 decreases approximately exponentially with the scale heights of ~10÷50 km and v_0 gradually increases from 0 to 7.9 km/s with increasing altitude z within the z~0 to 300 km altitude region, the scale L_1 mainly increases from $10 \div 10^2$ m at the ground to 10÷100 km in the ionospheric F region. Note that the derivation of the relation for L_1 is based on the fluid description that is applicable only to altitudes of less than 150÷200 km. The localized perturbations were observed by many researchers as far back as during the first rocket launches (end of the 1940s and beginning of the 1950s). The snow-plow effect also pertains to them [1].

For the first time, the large-scale perturbations were observed by Booker [2] during the launch of the Vanguard-II rocket from Cape Canaveral, Florida, U. S. A. at 11:00 EST on February 17, 1959. The release of hundreds of tons of water vapor H_2O and molecular hydrogen H_2 results in the exhaust-induced fast recombination of O^+ ions at a rate of $k=(2–3)\cdot10^{-14}$ m³/s. These phenomena are known as ionospheric holes. At altitudes near the F layer peak, their horizontal dimensions are of the order of ~1000 km, the vertical dimension is ~200 km (altitudes from 300 km to 500 km), and at their deepest point at z~400 km, holes represent ~95% depletion of electrons from the ambient level. The latter occurs for a period of a few minutes after the initial hole formation. It is important that the effects can persist for several hours [1]. The horizontal dimensions of ionospheric depletions increase with altitude and equal to ~10 to 1000 km at z~100 to 300 km, respectively.

Since that time such holes have been observed by many researchers (see, for instance, [3,4]). It should be added that the depletions in the ionosphere are accompanied by the generation of waves in the ionized gas with apparent velocities of V~0.1 to 1 km/s and periods of T~10 to 100 min.

Reviews of such disturbances have been presented by Karlov *et al.*, [5], Mendillo [6], Bernhardt [7], and Mendillo [1].

Apparently for the first time the global-scale perturbations in the ionosphere were observed by our research group after the launch of the Soyuz 19 spacecraft, while we participated in the Apollo-Soyuz Test Project on July 15, 1975. Then we used incoherent scatter radars at distances of about 1000 km from the launch site and ionosonde networks (see, for instance, [8]). During the launches of the U.S. Space Shuttle orbiters from the John Kennedy Space Center, Cape Canaveral, Florida, U. S. A., in particular, we have observed variations of plasma parameters in the D region, increases in the low-frequency cutoff f_{min} on the ionograms from 0.2 to 0.4 MHz (sometimes up to 1 MHz) and in the penetration frequencies $f_{o,x}F_2$ from 0.2 to 0.3 MHz, and their quasi-periodic oscillations [9].

Back in the 1970s, Rozumenko *et al.* [8] proposed a hypothesis that the geomagnetic micropulsations accompanying launches of rockets should cause the precipitation of energetic particles from the Van Allen radiation belts. Later, we have tried to confirm this assumption [8–11].

Since then our research group has observed perturbations from rocket launches in many clustered-instrument campaigns [10,11]. Until now, however, the mechanisms of perturbation transfer from rockets to the ionospheric regions at global-scale distances and characteristic features of its propagation in the ionosphere and magnetosphere are not completely clear. The purpose of this paper is to illustrate the observational capabilities of our equipment to investigate possible global-scale perturbations in the ionospheric D and F regions caused by a launch of the Space Shuttle orbiter. As an example, we consider the launch of the Space Shuttle orbiter Atlantis on May 15, 1997. A characteristic feature of these observations is that they were made at the beginning of the main phase of a geomagnetic storm. There is a reason to assume that the ionosphere-magnetosphere system becomes unstable during disturbances caused by natural processes, and, as a consequence, an anthropogenic source of energy of a relatively low power may become the cause of a sufficiently large perturbation. In other words, release of energy stored in the system can be triggered.

Equipment and Experimental Techniques

The lift-off of the Space Shuttle orbiter "Atlantis" took place from Cape Canaveral, Florida, U. S. A., at 08:07:062 UT on May 15, 1997. The total mass of the Shuttle system at lift-off is approximately 2 000 000 kg, the three Space Shuttle engines and the two solid-fuel rocket boosters generate 28 600 000 N of thrust at lift-off, a power of $P \sim 10^{11}$ W. Two solid rocket boosters have a thrust of 24,000,000 N at launch, burn for approximately 2 min, and separate from the external tank at ~ 50-km altitude; the three main propulsion rocket engines shut down at approximately 8 min 30 s mission elapsed time. The total energy release of all the engines is $E \sim 10^{14}$ J. For the first time, the orbital maneuvering system (OMS) engines ($F \sim 6 \cdot 10^4$ N, $P \sim 5 \cdot 10^8$ W, $E \sim 4 \cdot 10^{10}$ J) ignite at about 10.5 min mission elapsed time for about 1.5 min. The inclination of the orbit is 51.6°. The second burn of the OMS engines takes place at 44 min mission elapsed time for about 80 s at the ~300-km apogee point when the orbiter is over the eastern part of the Indian Ocean.

The diagnostic instruments are located at the Radiophysical Observatory of Kharkiv State University [11] in Eastern Ukraine at about 10 000 km from Cape Canaveral. The coordinates of the Radiophysical Observatory are shown in Table 1. The layout of the Observatory is presented in Fig. 1 where the electronics and antenna arrays are respectively designated by E and A: (1) *Cicada-M* receivers, (2) HF Doppler radar, (3) three-component magnetometer (M is a sensor), (4) partial reflection and spaced antenna radar (A4/1 is an $f = 1.5 \div 4.5$ MHz antenna, and A4/2 is an $f = 4.5 \div 15$ MHz antenna), (5) ionosonde, (6) transmitter and broadside two-row array of 15×30 m² of the bistatic HF radar for diagnostics of induced field-aligned irregularities in ionospheric heating experiments near N. Novgorod, Russia, (7) incoherent scatter radar; H is a hostel, C is a canteen, and G is a garage.

Table 1. *Coordinates of Kharkiv State University Radiophysical Observatory*

Geographic			Geomagnetic		Inclination	Declination, W	*L*
Elevation, m	Latitude, N	Longitude, E	Latitude, N	Longitude, E			
156	49°38'	36° 20'	45.37°	118.7°	66° 36.8'	6° 19.6'	≈2.0

Table 2. *Geophysical Conditions*

Date	10.7cm Radio Flux	SESC Sunspot Number	X-ray Flares			Estimated Planetary								
			C	M	X	A_P	K_P-indices							
12 May 97	72	12	1	0	0	3	1	0	1	1	1	2	1	1
13 May 97	74	15	0	0	0	3	0	0	0	0	1	2	2	1
14 May 97	74	17	0	0	0	6	1	0	0	1	2	3	3	2
15 May 97	73	15	0	0	0	53	3	3	6	7	7	5	3	2

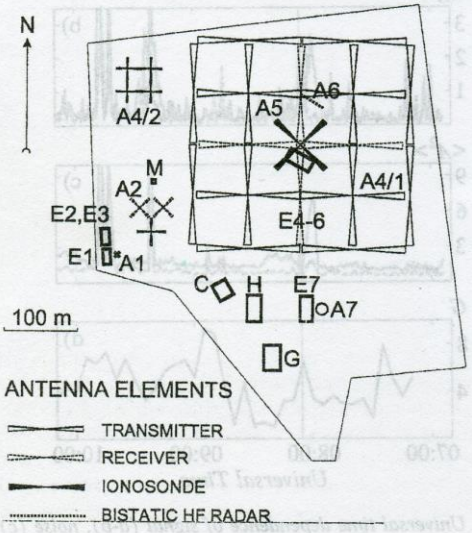

Fig. 1. *Layout of Radiophysical Observatory*

The Radiophysical Observatory is unique in Ukraine allowing the remote observations of ionospheric features and response over the altitude range from ~60 km to 1000 km simultaneously with magnetometer measurements.

In this study, we use measurements from the MF-HF partial reflection and HF Doppler radars. The ionosonde is used for monitoring the vertical structure of the ionosphere.

The partial reflection radar consists of a 150 kW 1.5÷15-MHz pulse transmitter, a vertically directed circularly polarized receiving array of two crossed double terminated rhombic antennas, a vertically directed 16-element linearly polarized transmitting antenna array of 300×300-m² aperture in the f = 1.5÷4.5 MHz frequency band and of 60×60-m² aperture in the f = 4.5÷15 MHz frequency band providing a gain of G≈1÷10 over an isotropic radiator. The τ = 25÷100 μs pulse lengths and the F_r=1÷10 per second pulse repetition rate are used; usually τ = 25 μs, providing approximately 3-km range resolution.

The receiver with an 86-dB dynamic range has an intermediate-frequency half-power bandwidth of 60 kHz, and a sensitivity of ~1 μV. To increase the signal-to-noise ratio, two to six samples of noise measurements are taken for each sounding pulse.

The two-channel wide bandwidth transmitter is of the master-oscillator, power-amplifier type with the modulator common to both channels. The digital synthesizer is used as a master oscillator. There is a possibility of the remote control of f, τ, and F_r.

The data acquisition, control, display, and storage functions are performed by a computer system. This equipment makes it possible to operate the radar in a "raw data mode", in which the raw receiver voltage samples of the amplitudes A_o and A_x of the ordinary and extraordinary, respectively, components of the wave partially reflected within the 45–105 km altitude range with a ~3-km altitude resolution are recorded on magnetic tape (dynamic range of 46 dB) for later processing and further analysis.

The HF Doppler radar used for this research is a two-channel system with the common master oscillator of 10^{-11} stability resulting in an additional signal processing gain from coherent Doppler integration. The Doppler measurement errors are ~0.01 Hz within the f_D=±5 Hz maximum Doppler frequency shift. The radar consists of a P=1 kW, τ=0.5 ms, pulse transmitter covering the f=1.5÷30 MHz frequency range at 0.01 Hz intervals at the F_r = 100÷200 per second pulse repetition rate. The transmitting and receiving terminated rhombic antennas provide a gain of G≈1÷10 over an isotropic radiator. The radar is usually operated in a mode of vertical incidence measurements, but sometimes it is used in a mode of receiving signals from oblique broadcast propagation paths.

Observations and Results

The observations were made from 06:00 UT to 15:00 UT on May 15, 1997. Observations made on other days of May of the same year are used as reference ones. The state of the ionosphere was characterized as quiet, and after 10:00 UT as weakly disturbed. The penetration frequency varied from 4.2 MHz to 5.1 MHz, and the low-frequency cutoff f_{min} on the ionograms varied from 1.2 MHz to 1.4 MHz.

According to solar event lists prepared by the U.S. Department of Commerce, NOAA, Space Environ-

ment Center, no solar events were observed during the interval of our observations on May 15, 1997; the 10.7 cm solar radio flux was 73 (in 10^{-22} W/m^2 Hz), and the sunspot number was 15. But geomagnetic activity was characterized as disturbed (see Table 2). The Shuttle was launched at the beginning of the main phase of the geomagnetic storm. The *Kp* index was increasing from 3 prior to the launch to 6 during the 3-hour interval (06:00 UT to 09:00 UT) which included the lift-off time (08:07:48.062 UT) and to 7 during the following two 3-hour intervals (09:00 UT to 15:00 UT).

Partial Reflections. The measurements of the amplitudes A_o and A_x of the ordinary and extraordinary components of the partially reflected wave and of noise A_{no} and A_{nx}, respectively, have been made at a frequency of 2.3 MHz. A sample of the universal time dependence of $<A^2_{o,x}>$ and $<A^2_{no,nx}>$ is shown in Figures 2(a) and 2(b) from 84 km and 81 km altitude, respectively, and that of noise is in Figures 2(c). The brackets < > designate the averaging over the data in segments of 1 minute in length at 1-min intervals. The root mean square errors of the estimates are of the order of 15%. Solid line is for the ordinary mode, dashed line is for the extraordinary mode. Here and in other Figures, the time of the lift-off (08:07 UT) is designated by the thin vertical line. Figures 2, a and 2, b show a significant increase (factor ~7) in $<A^2_{o,x}>$ in the interval following ~08:00 UT and between 09:00 UT and 10:00 UT. The same is true for $<A^2_{no,nx}>$ (see Fig. 2, c).

The $<A^2_o>$ data in segments of Δt_2 = 32 min in length, centered on the time indicated in Fig. 2, d, and taken at Δt_1=5 min intervals have been subjected to a spectral analysis, and the spectral components have been normalized to the root-mean-square $<A^2_o>$ variations estimated on the same segments. The results show that the 5.3-min component variations from 84 km altitude (see Fig. 2, d) exhibit the greatest increase (factor 2 – 3).

For the first time, we observed approximately the same periods by the partial reflection technique back in the 1980s, and almost the same periods have been observed by many other researchers; one of the recent such studies has been made by Pan *et al.* [12] in the polar mesosphere. Apparently, these features may be ascribed to internal gravity wave dissipation, momentum deposition, and turbulence generation. Notice that the T = 5 min period is approximately equal to the characteristic period of oscillations in the mesosphere. Under adiabatic conditions, in an isothermal atmosphere, the buoyancy period is given by (see, for instance, [13])

$$T = 2\pi\sqrt{\frac{H}{g}\frac{\gamma}{\gamma-1}}$$

where g is the gravitational acceleration, H is the scale height, γ is the ratio of the specific heats at constant pressure and constant volume.

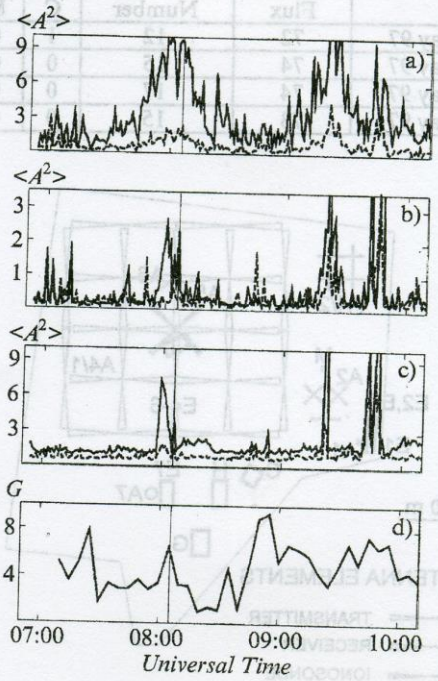

Fig. 2. *Universal time dependence of signal (a-b), noise (c), and 5.3-min period spectral component (d) (everything in relative units)*

The dependence

$$R(z) = \frac{< A_x^2 > - < A_{nx}^2 >}{< A_o^2 > - < A_{nc}^2 >}$$

is the basis for obtaining $N(z)$ profiles by the technique of differential absorption. The amplitudes are being averaged over 5÷10 min intervals.

The theory of partial reflection yields the following relation between the $R(z)$ profile estimated from the measurements and the $N(z)$ electron number density profile which should be determined:

$$\ln\frac{R_0(z)}{R(z)} = \int_{z_0}^{z} K(z', \nu(z'))N(z')dz' \qquad (1)$$

where $K(z')$ is the kernel of the integral equation, $R_0(z)$ is the function known from the theory of the partial reflection technique, z_0 is the altitude of the

lower edge of the ionosphere, ν is the electron collision frequency.

Formerly, $N(z)$ profiles were derived by differentiating (1) with respect to z, yielding

$$N(z)=K^{-1}(z)\frac{d\tilde{R}}{dz}, \qquad \tilde{R}=\ln\frac{R_0}{R}. \qquad (2)$$

The quality of the profiles obtained depends on random errors in $<A^2_{o,x}>$ and $<A^2_{no,nx}>$ estimates, as well as on the stability of an algorithm of numerical differentiation caused by measurement errors in $R(z)$.

Since the inversion problem of the partial reflection technique is ill-posed, the Tikhonov regularization solution obtained in [14] has been used in this study. The collision frequency profile is assumed to be that of Gurevich [15]. The essence of the algorithm is as follows.

Instead of using (2), the algorithm of regularization have been designed to determine $N(z)$ by minimizing the functional:

$$\Phi[N,\tilde{R},\tilde{\alpha}]=\left\|\int_{z_0}^{z}K(z')N(z')\,dz'-\tilde{R}(z)\right\|^2+\tilde{\alpha}\tilde{\Omega}[N] \qquad (3)$$

where $\tilde{\alpha}$ is the parameter of regularization, $\tilde{\Omega}$ is the stabilizer.

In this work, the stabilizer is chosen to have the form:

$$\tilde{\Omega}[N]=\left\|\left(N/\tilde{N}-1\right)\left(q_{\max}/q\right)^{1/4}\right\|^2,$$

$$q^{-1}=q_o^{-1}+q_x^{-1}, \quad q_{\max}=\max\{q(z)\}.$$

Here, $q_{o,x}=<A^2_{o,x}>/<A^2_{no,nx}>$ is the signal-to-noise ratio for o- and x-waves, respectively, $\tilde{N}(z)$ is the initial approximation to $N(z)$.

Note that the dependence of the stabilizer $\tilde{\Omega}$ on $N(z)$ is not very strong and weakens the effects of the data obtained from the altitudes where $q_{o,x}$ are small. The application of this regularization algorithm results in the reduction (factor 3 – 5) of the effects of measurement errors on the restoration of $N(z)$ from $\tilde{R}(z)$ and in the extension of the altitude range by approximately 10 km. Errors in the estimates of $<A^2_{o,x}>$ rise significantly with decreasing of the smoothing interval ΔT on the one hand, and the variations in N are difficult to follow with increasing of the ΔT on the other hand. As a result, the optimization of estimating the $<A^2_{o,x}>$ is achieved on ΔT intervals of order 5÷10 min.

Errors in the $N(z)$ profiles derived on the basis of algorithm (3) decrease from 50 % to 30 % when the integration time increases from 5 to 10 min, respectively. We have obtained N profiles in the altitude range of z~75÷85 km; at higher and lower altitudes, the signal-to-noise ratios are too small ($q_{o,x}<1$). Figure 3 shows universal time dependence of the electron number density (solid line for May 15, 1997; dashed line for May 24, 1997): (a) at 84 km altitude; (b) at 81 km altitude; (c) at 78 km altitude; (d) at 75 km altitude. It can be seen that until 08:50 UT on May 15, 1997, N remains almost unchanged. At about 08:50 UT, quasi-periodic 30 % to 70 % variations in N with the period of T=30 min ensued at ~75 to 85 km and persisted for T≈2 hours. The root mean square errors of the estimates are of the order of 30%. If these variations were caused by the launch of the rocket, then the time delays between the onset of the perturbations at different altitudes and the launch time should be approximately 45 to 55 min. It is worth noting that such quasi-periodic perturbations did not appear on a reference day (dashed lines in Fig. 3).

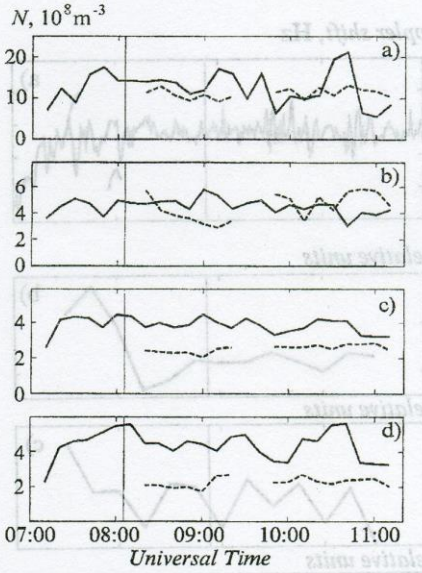

Fig. 3. *Universal time dependence of the electron number density*

Doppler Shift. The measurements have been made at 4.1 MHz and at vertical incidence. The available data in segments of Δt_1=51.2 s in length were subjected to a spectral analysis, and the Doppler spectra were estimated with approximate 0.02-Hz frequency resolution. Sample Doppler spectra are presented in Figure 4: (a) before the lift-off and during the first minutes after it; (b) the appearance of an additional component and quasi-periodic variations in f_D; (c) quasi-periodic variations in the f_D spectrum and the destruction of the spectra. The horizontal bars at the right-

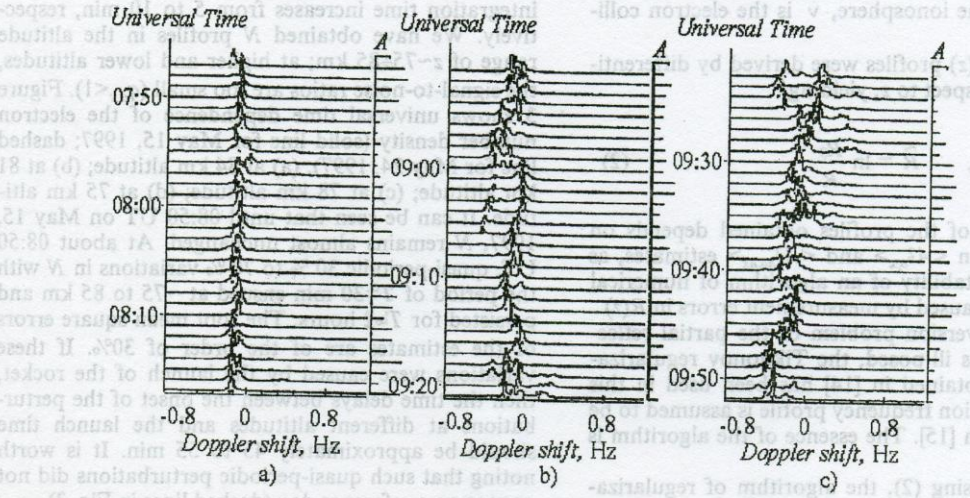

Fig. 4. *Sample Doppler spectra (A in relative units)*

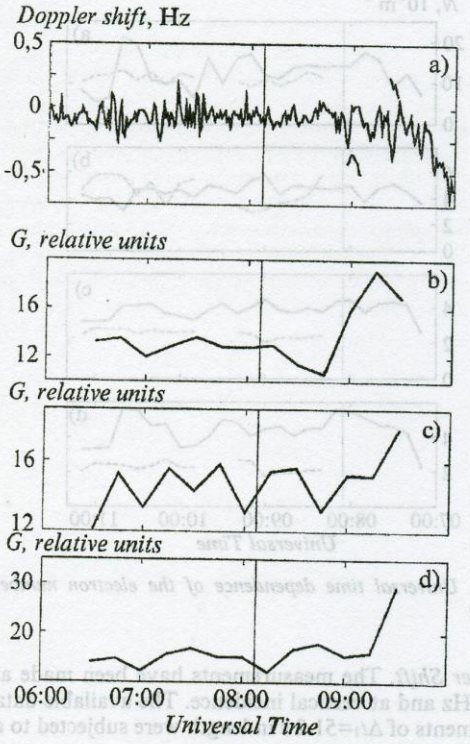

Fig. 5. *Universal time dependence of (a) the principal component in the f_D spectrum and its harmonics (b-d)*

hand side of each spectrum signify magnitude of the signal relative amplitude. The analysis of the data shows that the echo signal contains components with different Doppler shifts. The examination of the spectra in Fig. 4(a) reveals that the main component has approximately 0.1 to 0.2 Hz half-power spectral width before ~ 08:07 UT; at 08:54 UT, two peaks appear with a difference in the Doppler shifts of approximately 0.4 Hz and exist for about ~10 min (Fig. 4(b). Next time, two peaks exist in the spectrum from 09:18 UT to 09:27 UT. For the rest of the time interval, the Doppler shift widens up to 0.4 Hz (Figures 4(b) and 4(c)). Figure 5 shows universal time dependence of (a) the principal component in the f_D spectrum and its harmonics with the period of (b) $T\approx12.8$ min, (c) T=32 min, and (d) T=64 min. The analysis was carried out on the data in segments of 64 min in length, centered on the time indicated. From the dependence in Fig. 5(a), it follows that from 06:00 UT to 08:00 UT the magnitude of variations does not exceed $\Delta f_D \approx \pm 0.2$ Hz with an average of about $\bar{f}_D \approx -0.1$ Hz. During the 08:00÷8:40 UT period, $\bar{f}_D \approx -0.1$ Hz, and $\Delta f_D \approx 0.1$ Hz, after 08:50 UT, $\bar{f}_D$ smoothly decreases to –0.7 Hz during a 70-min interval. Quasi-periodic perturbations with quasi-periods of tens of minutes are superimposed on this $f_D(t)$ dependence. A spectral analysis method applied to the Δt_2 = 64 min data segments at 15 min intervals has revealed the major increase in a wave process with the T=13 min period on the F-region heights of z~250÷300 km at about 08:50 UT (Fig. 5(b)). Thus, before 08:00÷08:10 UT the amplitude of this component is approximately 0.1 Hz, and in 40 to 100 min after it, this component is found to be 0.2÷0.3 Hz. The amplitudes of the components with T=32 min and T=64 min increase by tens per cent. Quasi-

periodic perturbations persist for not less than 1 hour. It is interesting to note that the time delays of the perturbations are approximately 45÷50 min, i. e. they are about the same as in the lower ionosphere.

Discussion

First, consider the processes acting in the lower ionosphere. Here, quasi-periodic perturbations in N observed at $z \sim 75 \div 85$ km approximately from 09:00 UT to 11:00 UT exhibit T=30 min and $\Delta N/N_0 = 30 \div 70$ %. It is unlikely that such sufficiently large perturbations are caused by the propagation of waves in the lower ionosphere. It is more probable that they are caused by pulsating fluxes of energetic particles precipitating from the magnetosphere. If it is so, consider the estimates of their parameters.

The power flux of precipitating particles is equal to [16]

$$\Pi = \varepsilon p = 2\,\varepsilon_i\,\Delta z\,\Delta q_i \qquad (4)$$

where p is the flux of the primary particles responsible for ionization, Δq_i is the change in the production rate per unit volume of positive ions resulting from the ionization of neutral atmospheric constituents, $\Delta z \approx 10$ km is the thickness of the region where the precipitating particles are absorbed, ε is the energy of the primary particles, $\varepsilon_i \approx 5 \cdot 10^{-18}$ J is the mean energy loss per ion pair formed.

First, let us calculate Δq_i. The steady-state solution is

$$q_{i0} = \alpha N_0^2, \qquad q_i = \alpha N^2$$

where α is the effective ion-electron recombination rate coefficient for the positive ions, N_0 is the undisturbed electron number density, N is the disturbed electron number density, q_{i0} is the undisturbed total production rate per unit volume of positive ions resulting from the ionization of neutral atmospheric constituents, q_i is the disturbed total production rate per unit volume of positive ions resulting from the ionization of neutral atmospheric constituents.

Then

$$\Delta q_i = q_i - q_{i0} = \alpha(N^2 - N_0^2) = \alpha N_0^2 \left(\frac{N^2}{N_0^2} - 1\right). \qquad (5)$$

At $z \le 75$ km, let the predominant type of recombination be a cluster-ion recombination with $\alpha \approx 10^{-11}$ m^{3}s^{-1}, and above 100 km, let it be a molecular ion recombination with $\alpha \approx 2 \cdot 10^{-13}$ m^3 s^{-1}. Between these regions, α gradually decreases from 10^{-11} to $2 \cdot 10^{-13}$ m^3 s^{-1}. From (4) and (5) it follows that

$$\Pi = 2\varepsilon_i \Delta z \alpha_0 N_0^2 \left(\frac{N^2}{N_0^2} - 1\right) = 2\varepsilon_i \Delta z\, q_{i0} \left(\frac{N^2}{N_0^2} - 1\right). \qquad (6)$$

Our estimates of ε and p for electrons (denoted by the subscript 'e'), Π and other parameters obtained from relations (4), (5), and (6) are presented in Table 3. The results show that the quasi-periodic oscillation of the electron number density N observed in the lower ionosphere can be caused by the fluxes of 10^2- to 10-keV electrons pulsating from $\sim 10^6$ m^{-2} s^{-1} to $4 \cdot 10^7$ m^{-2} s^{-1}. It should be added that such values of p_e are not great for the middle latitude ionosphere. At high latitudes, p_e is a few orders of magnitude greater (see, for instance, [16]). Let us estimate the power P_e and energy E_e of the fluxes of electrons precipitating presumably over an area of $S_e = 10^{14}$ m^2 for $\Delta t_e = 5 \cdot 10^3$ s. Introducing this assumption,

$$P_e = \Pi S_e, \qquad E_e = P_e \Delta t_e.$$

Then for $\Pi \sim 10^{-8} \div 4 \cdot 10^{-8}$ J/m^{2}s, we have $P_e \approx (1 \div 4) \cdot 10^6$ W, $E_e \approx 5 \cdot 10^9 \div 2 \cdot 10^{10}$ J. If precipitating particles are protons with $\varepsilon_p \sim 1$–5 MeV, then $p_p \sim 10^5$ m^{-2} s^{-1}.

For $E_e = 5 \cdot 10^9 \div 2 \cdot 10^{10}$ J and $E \sim 4 \cdot 10^{10}$ J, we have $\eta = E_e / E \sim 0.1 \div 0.5$.

Next consider the processes acting in the ionospheric F region and make an estimate of the amplitudes of quasi-periodic perturbations in N.

For vertical incidence at the ionosphere, the Doppler shift is given by (see, for instance, [17]):

$$\frac{f_D}{f} = -\frac{2}{c}\frac{\mathrm{d}}{\mathrm{d}t}\int_{z_0}^{z_r} n(t,z)\,\mathrm{d}z \qquad (7)$$

where c is the free space speed of light, n is the plasma refractive index, z_r is the reflection altitude.

Table 3. Parameters of the ionosphere and precipitating particles.

z, km	α, m^{3}s^{-1}	N_0, m^{-3}	N, m^{-3}	q_{i0}, m^{-3} s^{-1}	Δq_i, m^{-3} s^{-1}	Π, Jm^{-2}s^{-1}	ε_e, keV	p_e, m^{-2}s^{-1}
75	10^{-11}	$3 \cdot 10^8$	$4 \cdot 10^8$	$9 \cdot 10^5$	$7 \cdot 10^5$	$1.4 \cdot 10^{-8}$	10^2	$1.4 \cdot 10^6$
78	$5 \cdot 10^{-12}$	$3 \cdot 10^8$	$4 \cdot 10^8$	$4.5 \cdot 10^5$	$3.5 \cdot 10^5$	$7 \cdot 10^{-9}$	50	$1.4 \cdot 10^6$
81	$2 \cdot 10^{-12}$	$5 \cdot 10^8$	$6 \cdot 10^8$	$5 \cdot 10^5$	$2.2 \cdot 10^5$	$4.4 \cdot 10^{-9}$	20	$2.2 \cdot 10^6$
84	10^{-12}	10^9	$1.7 \cdot 10^9$	10^6	$2 \cdot 10^6$	$4 \cdot 10^{-8}$	10	$4 \cdot 10^7$

Provided the effects of magnetic field and particle collisions can be neglected,

$$n^2 = 1 - \frac{f_p^2}{f^2}. \qquad (8)$$

Here f_p is the electron plasma frequency.

To model the $N(z)$ profile of the ionospheric F region, we use a parabola with the maximum of $N = N_m$ and the half-thickness of l. The propagation of a quasi-periodic perturbation with a period of T and a frequency of $\Omega = 2\pi/T$ results in the modulation of N observed in the F region. To simplify the following estimates, we suppose that $\Delta N/N$ does not depend on altitude. Then,

$$N(t,z) = N_m\left[1-\left(\frac{z-z_m}{l}\right)^2\right]\left(1+\frac{\Delta N}{N_m}\sin\Omega t\right),$$
$$f_p^2(t,z) = f_{pm}^2\left[1-\left(\frac{z-z_m}{l}\right)^2\right]\left(1+\frac{\Delta N}{N_m}\sin\Omega t\right) \qquad (9)$$

where f_{pm} is the plasma frequency at the $N(z)$ profile peak altitude z_m.

Defining the phase path in relation (7) as

$$s_p = \int_{z_0}^{z_r} n\,dz \qquad (10)$$

and substituting (8) and (9) in (10) yields

$$s_p = \frac{l}{2}y(\beta), \qquad y(\beta) = 1-\frac{1}{2}\cdot\frac{\beta^2-1}{\beta}\ln\frac{\beta+1}{\beta-1}$$

where:

$$\beta = \frac{f_{pm}}{f}\left(1+\frac{\Delta N}{N}\sin\Omega t\right)^{1/2}.$$

From (7) and (11), we have

$$\frac{f_D}{f} = -\frac{2}{c}\frac{ds_p}{d\beta}\frac{d\beta}{dt} = -\frac{l}{c}y'(\beta)\beta'. \qquad (12)$$

Here

$$y'(\beta) = \frac{dy}{d\beta} = \frac{1}{\beta} - \frac{\beta^2+1}{2\beta^2}\ln\frac{\beta+1}{\beta-1},$$

$$\beta' = \frac{d\beta}{dt} = \frac{f_{pm}}{2f}\left(1+\frac{\Delta N}{N}\sin\Omega t\right)^{-1/2}\frac{\Delta N}{N_m}\Omega\cos\Omega t.$$

Since in the F region $\Delta N/N_m << 1$, it follows that $\beta \approx \beta_0 = f_{pm}/f$. Then

$$y'(\beta) \approx y'(\beta_0),$$

$$\beta' \approx \frac{\Omega}{2}\beta_0\frac{\Delta N}{N_m}\cos\Omega t = \frac{\pi}{T}\beta_0\frac{\Delta N}{N_m}\cos\Omega t.$$

From (12) it follows that

$$\frac{f_D}{f} \approx \pi\frac{l}{cT}\frac{\Delta N}{N_m}y'(\beta_0)\beta_0\cos\Omega t.$$

For the amplitude of f_{D_0} we have

$$f_{D0} = \pi\frac{l}{cT}\frac{\Delta N}{N_m}\left|y'(\beta_0)\right|f_{pm},$$

from which it follows that

$$\frac{\Delta N}{N_m} = \frac{1}{\pi}\frac{f_{D0}}{f_{pm}}\frac{cT}{l}\left|y'(\beta_0)\right|^{-1}. \qquad (13)$$

For the May 15, 1997, experiment, $f_{pm} \approx$ 5 MHz, l= 200 km, $f_{D_0} \approx 0.25$ Hz, $T \approx 800$ s, $y'(\beta_0) \approx 0.85$. Then from (13), $\Delta N/N_m \approx 2\%$.

Thus, the quasi-periodic perturbation appearing in the F region has a significantly smaller (factor 15 – 35) relative amplitude than that observed in the D region, although this perturbation begins actually simultaneously with the quasi-periodic perturbation in the lower ionosphere.

Note that such waves originate at high latitudes during geomagnetic storms and propagate from high to low latitudes at a velocity of about 1 km/s [18]. Provided the wave had passed the distance of R=3 000÷4 000 km, it should be originated at high latitudes ~ 50 to 70 min before the detection of the quasi-periodic perturbations at about 08:50 UT to 08:55 UT. That is the very moment of beginning of the main phase of geomagnetic storm.

At the same time, it should be noted [18] that the quasi-periodic processes in the ionosphere with T~10 to 100 min originate from (or, more precisely, are enhanced by) earthquakes, explosions, and other disturbances.

It is unlikely that the observed quasi-periodic perturbations are caused by the main engine burn because it takes place mainly in the near-earth atmosphere, and the part of energy transformed into the

ionospheric perturbations is negligibly small. With a delay of approximately 50 min, their apparent velocity would be V~3 km/s. But the perturbations could in principle be caused by the second Shuttle OMS engine burn which took place at 44 min mission elapsed time at the ~300-km apogee point. If this is true, then the time delay obtained from $f_D(t)$ data is 7±2 min, and for $R \approx 12{,}000$ km we have $V \approx 30 \pm 10$ km/s. Although the Shuttle OMS engine power has a value a factor of hundreds lower, and their energy release has a value a factor of thousands lower than that of the main engines, the perturbations in the ionosphere from the Shuttle OMS engine burn might be significant. This is caused by the fact that the energy release takes place at ~300-km altitude in the ionosphere rather than in the near-earth atmosphere.

To which extent are the velocities of V=20÷40 km/s reasonable? These magnitudes are considerably greater than the speed of sound (0.3÷0.7 km/s) and the velocities of slow MHD waves (~1÷3 km/s) (see [18]). At the same time, these values of V are significantly less than the velocities of MHD waves in the magnetosphere (~1 000 km/s) and the free space speed of light. However, one should have in mind that V is an apparent velocity. It approaches to the observed magnitude if the temporal evolution of the process associated with the precipitation of energetic particles or other processes acting in the ionosphere are much slower than the process of propagation of the quasi-periodic perturbations. Nevertheless, our estimates of V are completely in agreement with Sorokin's estimates [19]. Exactly the same velocities of the order of tens kilometers per second are observed during rocket launches, powerful explosions, earthquakes, magnetospheric disturbances, etc. Such processes are accompanied by wave-driven perturbations in the magnetosphere-ionosphere system in which the geomagnetic field plays a key role. These waves are called "gyrotropic" waves and have been studied in detail by Sorokin and Fedorovich [20].

It seems unlikely that the perturbations observed are transferred from the magnetically conjugate ionosphere which the Space Shuttle crossed at about 08:40 UT to 08:45 UT without a Shuttle OMS engine burn.

Thus, the launch of the space vehicle with the geomagnetic storm at the background has significantly complicated detecting possible ionospheric effects caused by the anthropogenic influence. The effects in question do not in principle differ from natural plasma phenomena. Effects caused by rocket launch, or, more precisely, caused by Shuttle OMS engine burns may be associated with the generation of quasi-periodic perturbations in the D and F regions. However, such processes could also be induced by the geomagnetic storm. A complicated chain of cause and effect is presently not well understood in order to determine the principal reasons why Shuttle OMS engine burns result in energetic particle precipitation from the magnetosphere. In general, the following scheme could be adopted. A plasma jet in the ionosphere generates MHD waves which reach the magnetosphere, couple with the particles trapped in the radiation belts, and cause their precipitation into the Earth's atmosphere. However, the data set acquired at present does not allow us to distinguish between the effects caused by the storm and the launch.

Conclusions

1. The observations of global-scale perturbations in the ionosphere are made simultaneously with the launch of the Space Shuttle orbiter Atlantis at a range of ~10 000 km from the launch site. The launch took place at the beginning of the main phase of the geomagnetic storm on May 15, 1997.

2. In 45 to 50 min after the launch of the Space Shuttle (i. e. at about 08:50 UT), a quasi-periodic oscillation of the D-region densities with a 30-min period and a quasi-periodic oscillation of the F-region densities with a 13-min period appeared and persisted for 1 to 2 hours.

3. The quasi-periodic oscillations of the D-region densities with $\Delta N/N_0$ ~30÷70 % could be caused by the varying 10^2÷10-keV electron fluxes of 10^5 $m^{-2}s^{-1}$ or 1÷5 MeV proton fluxes of ~10^6÷$4 \cdot 10^7$ $m^{-2}s^{-1}$. Provided the precipitation was on a global scale, their power and energy could be ~ 1 to 4 MW and 5 to 20 GJ, respectively.

4. The relatively weak quasi-periodic variations of the Doppler shift with a 13-min period could be caused by the enhancements of quasi-periodic perturbations in the electron number density with an amplitude of about 2 %.

5. It is impossible now to determine uniquely whether the observed ionospheric oscillations were related to the launch of the space vehicle or were the result of a propagating ionospheric disturbance launched by the geomagnetic storm. At the same time, the possibility cannot be excluded that the geomagnetic storm enhanced the perturbations from the Shuttle OMS engine burn at ~300 km.

Acknowledgments. The authors have been supported by Science and Technology Center in Ukraine Grant No. 471.

References

1. M. Mendillo. Adv. Space Res. 1988, **8**, No. 1, pp. 51-62.
2. H. G. Booker. J. Geophys. Res. 1961, **66**, No. A4, pp. 1073-1079.
3. M. Mendillo, G. S. Hawkins, and J. A. Klobuchar. J. Geophys. Res. 1975, **80**, No. 6, pp. 2217-2228.

4. G. F. Zasov, V. D. Karlov, T. E. Romanchuk, G. N. Tkachev, and M. G. Trukhan. Geomagnetism and Aeronomy. 1977, **17**, No. 2, pp. 346-348 (in Russian).
5. V. D. Karlov, S. I. Kozlov, and G. N. Tkachev. Kosmicheskie Issledovaniya. 1980, **18**, No. 2, pp. 266-277 (in Russian).
6. M. Mendillo. In: Proc. Int. Symp. Active Exp. Space. Paris, 1983, pp. 285-292.
7. P. A. Bernhardt. J. Geophys. Res. 1987, **92**, No. A5, pp. 4617-4628.
8. V. T. Rozumenko, L. S. Kostrov, S. I. Martynenko, V. A. Misyura, O. F. Tyrnov, A. M. Tsymbal, and L. F. Chernogor. Turkish J. of Physics. 1994, **18**, No. 11, pp. 1193-1198.
9. V. A. Misiura, L. A. Piven, O. V. Pakhomova, and L. F. Chernogor. Geomagnetism and Aeronomy. 1987, **27**, No. 4, pp. 677-679 (in Russian).
10. A. I. Gritchin, V. L. Dorohov, I. I. Kapanin, A. I. Karpachev, L. S. Kostrov, S. G. Leus, S. I. Martynenko, N. N. Mashtaler, Yu. B. Milovanov, V. A. Misyura, O. V. Pakhomova, V. A. Podnos, S. N. Pokhil'ko, E. N. Protopop, V. T. Rozumenko, V. G. Somov, O. F. Tyrnov, V. N. Fedorenko, Yu. P. Fedorenko, A. M. Tsymbal, L. F. Chernogor, S. G. Chulakov, and A. S. Shemet. In: Space Plasma Physics. Proceedings of International Seminar (1993, Kiev, Ukraine). Kiev: NSAU, 1994, pp. 161-170.
11. O. F. Tyrnov, K. P. Garmash, A. M. Gokov, A. I. Gritchin, V. L. Dorohov, L. G. Kontzevaya, L. S. Kostrov, S. G. Leus, S. I. Martynenko, V. A. Misyura, V. A. Podnos, S. N. Pokhil'ko, V. T. Rozumenko, V. G. Somov, A. M. Tsymbal, L. F. Chernogor, and A. S. Shemet. Turkish J. of Physics. 1994, **18**, No. 11, pp. 1260-1265.
12. C. J. Pan, C. H. Liu, J. Y. Liu, and Roettger. J. Abstract Book. 8th Scientific Assembly of IAGA with ICMA and STP Symposia. Uppsala, IAGA. 1997, p. 198.
13. E. E. Gossard and W. H. Hooke. Waves in the Atmosphere. Elsevier Publishing Co., Inc., New York., 1975, 532 pp.
14. K. P. Garmash and L. F. Chernogor. Geomagnetism and Aeronomy. 1996, **36**, No. 2, pp. 75-81 (in Russian).
15. A. V. Gurevich. Nonlinear Phenomena in the Ionosphere. Springer-Verlag, New York, 1978, X, 366 pp.
16. W. B. Lyatsky and Yu. P. Maltsev. Magnetosphere-ionosphere coupling. Nauka, Moscow, 1983, 192 pp. (in Russian).
17. K. Davies. Ionospheric Radio. Peter Peregrinus Ltd., London, 1990. XX, 580 pp.
18. V. M. Sorokin and G. V. Fedorovich. Physics of Slow MHD Waves in the Ionospheric Plasma. Energoatomizdat, Moscow, 1982, 136 pp. (in Russian).
19. V. M. Sorokin. Bulletin of Kharkiv Polytechnic Institute. Investigations of the ionosphere by incoherent scatter radar. 1989, No. 271, Issue 7, pp. 29–39 (in Russian).
20. V. M. Sorokin and G. V. Fedorovich. Izv. Vuzov. Radio Physics. 1982, **25**, No. 5, pp. 495-507 (in Russian).

Возмущения в ионосфере в день старта мощного американского космического корабля

Л. Ф. Черногор, К. П. Гармаш, Л. С. Костров, В. Т. Розуменко, О. Ф. Тырнов, А. М. Цымбал

Обнаружены квазипериодические возмущения концентрации электронов как в D-, так и в F-областях в день старта космического аппарата "Атлантис" 15 мая 1997 г., по времени совпадающего с началом главной фазы магнитной бури. Величина квазипериодов – десятки минут, продолжительность – 1÷2 ч. Делается попытка связать наблюдаемые возмущения с возможными глобальными процессами в нижней и средней ионосфере, сопутствующими старту и полету космического аппарата.

Збурення в іоносфері в день запуску потужного американського космічного корабля

Л. Ф. Чорногор, К. П. Гармаш, Л. С. Костров, В. Т. Розуменко, О. Ф. Тирнов, А. М. Цимбал

Виявлено квазіперіодичні збурення електронної концентрації як у шарі D, так і у шарі F іоносфери у день старту космічного човна "Атлантис" 15 травня 1997 р., який співпадає за часом з початком головної фази магнітної бурі. Величини квазіперіодів – десятки хвилин, тривалість – 1÷2 год. Робиться спроба пов'язати спостережені збурення з можливими глобальними процесами в нижній та середній іоносфері, які супроводжують старт та політ космічного апарата.